Journal of Dental Research
2018, Vol. 97(8) 937–945

DOI: 10.1177/0022034518759295
journals.sagepub.com/home/jdr

Reduced Orthodontic Tooth Movement in *Enpp1* Mutant Mice with Hypercementosis

M. Wolf[1,2], M. Ao[2], M.B. Chavez[3], T.N. Kolli[3], V. Thumbigere-Math[2,4], K. Becker[5], E.Y. Chu[2], A. Jäger[6], M.J. Somerman[2], and B.L. Foster[3]

Abstract

Previous studies revealed that cementum formation is tightly regulated by inorganic pyrophosphate (PP_i), a mineralization inhibitor. Local PP_i concentrations are determined by regulators, including ectonucleotide pyrophosphatase/phosphodiesterase 1 (ENPP1), which increases PP_i concentrations by adenosine triphosphate hydrolysis. Orthodontic forces stimulate alveolar bone remodelling, leading to orthodontic tooth movement (OTM). To better understand how disturbed mineral metabolism and the resulting altered periodontal structures affect OTM, we employed *Enpp1* mutant mice that feature reduced PP_i and increased cervical cementum in a model of OTM induced by a stretched closed-coil spring ligated between the maxillary left first molar and maxillary incisors. We analyzed tooth movement, osteoclast/odontoclast response, and tooth root resorption by micro–computed tomography, histology, histomorphometry, and immunohistochemistry. Preoperatively, we noted an altered periodontium in *Enpp1* mutant mice, with significantly increased periodontal ligament (PDL) volume and thickness, as well as increased PDL-bone/tooth root surface area, compared to wild-type (WT) controls. After 11 d of orthodontic treatment, *Enpp1* mutant mice displayed 38% reduced tooth movement versus WT mice. Molar roots in *Enpp1* mutant mice exhibited less change in PDL width in compression and tension zones compared to WT mice. Root resorption was noted in both groups with no difference in average depths, but resorption lacunae in *Enpp1* mutant mice were almost entirely limited to cementum, with 150% increased cementum resorption and 92% decreased dentin resorption. Osteoclast/odontoclast cells were reduced by 64% in *Enpp1* mutant mice, with a predominance of tartrate-resistant acid phosphatase (TRAP)–positive cells on root surfaces, compared to WT mice. Increased numbers of TRAP-positive cells on root surfaces were associated with robust immunolocalization of osteopontin (OPN) and receptor-activator of NF-κB ligand (RANKL). Collectively, reduced response to orthodontic forces, decreased tooth movement, and altered osteoclast/odontoclast distribution suggests *Enpp1* loss of function has direct effects on clastic function/recruitment and/or indirect effects on periodontal remodeling via altered periodontal structure or tissue mineralization.

Keywords: dental cementum, tooth calcification, dentin, orthodontics, osteoclasts, bone

Introduction

During orthodontic tooth movement (OTM), mechanical forces trigger stress/strain distribution in the periodontal ligament (PDL), initiating a signaling cascade resulting in alveolar bone remodeling allowing for tooth movement. Localized vascular disturbances and cell stress evoke cell necrosis, initiating a host immune response, including chemoattraction of immune-competent cells and their differentiation along the monocyte/macrophage lineage, to clear cellular debris and facilitate structural reorganization of the periodontium in the first stage and tooth movement in the later stage (Jäger et al. 1993; Kim et al. 2010; Wolf et al. 2016). However, excessive orthodontic forces or immune responses sometimes lead to adverse effects, including loss of alveolar bone height and external tooth root resorption of cementum and dentin by osteoclast/odontoclast cells (Yamaguchi et al. 2006; Koide et al. 2010).

Predictable repair and regeneration of periodontal tissues are major unrealized goals of periodontal therapy (Bosshardt and Sculean 2009), including cases of OTM-associated root resorption. There is continued interest in better understanding molecular regulators of cementogenesis and how these might restrict the magnitude of root resorption and/or promote

[1]Department of Orthodontics, Aachen University, Aachen, Germany
[2]National Institute of Arthritis and Musculoskeletal and Skin Diseases (NIAMS), National Institutes of Health (NIH), Bethesda, MD, USA
[3]Division of Biosciences, College of Dentistry, The Ohio State University, Columbus, OH, USA
[4]Division of Periodontics, School of Dentistry, University of Maryland, Baltimore, MD, USA
[5]Department of Orthodontics, Universitätsklinikum Düsseldorf, Düsseldorf, Germany
[6]Department of Orthodontics, University of Bonn, Bonn, Germany

A supplemental appendix to this article is available online.

Corresponding Author:
B.L. Foster, Division of Biosciences, College of Dentistry, The Ohio State University, 4163 Postle Hall, 305 W. 12th Avenue, Columbus, OH 43210, USA.
Email: foster.1004@osu.edu

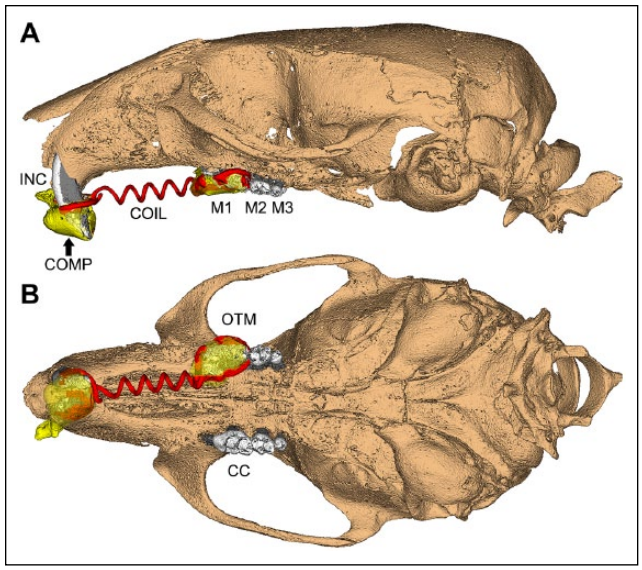

Figure 1. Orthodontic apparatus employed in mouse maxillae. Schematic based on micro–computed tomography scan showing 3-dimensional (**A**) sagittal and (**B**) occlusal views of an orthodontic appliance used in mouse maxillae in this study. A super elastic coil spring (COIL; shaded red) was fixed between the maxillary left first molar (M1) and maxillary incisors (INC) using a dental composite (COMP; shaded yellow) to achieve mesial (anterior) M1 movement. The loaded side is labeled as the orthodontic tooth movement (OTM) side, while the contralateral control (CC) side received no orthodontic appliance (split-mouth design). M2 = second molar; M3 = third molar.

reparative cementum formation. Studies in mice revealed cementum to be exceptionally sensitive to regulation by inorganic pyrophosphate (PP_i), a mineralization inhibitor. Local PP_i concentrations are determined by factors including tissue-nonspecific alkaline phosphatase (gene: *Alpl*; protein: TNAP), which hydrolyzes PP_i to promote mineralization; progressive ankylosis protein (*Ank*; ANK), which regulates PP_i transport to the extracellular space; and ectonucleotide pyrophosphatase/phosphodiesterase 1 (*Enpp1*; ENPP1), which hydrolyzes adenosine triphosphate (ATP) to PP_i (Millán 2013). Reduction of PP_i by loss of function of *Ank* or *Enpp1* in mice results in hypermineralization, including ectopic calcification of joints and soft tissues (Harmey et al. 2004; Millán 2013). In dentoalveolar tissues, *Ank* or *Enpp1* loss of function increases acellular cementum (Nociti et al. 2002; Foster et al. 2012; Zweifler et al. 2015; Thumbigere-Math et al. 2018). Studies employing surgical fenestration defects in *Ank* knockout mice revealed that genetically reducing PP_i enhanced cementum repair (Rodrigues et al. 2011). However, how reduced PP_i would alter periodontal remodeling in response to OTM has remained unexplored.

We hypothesized that altered mineral metabolism in *Enpp1* mutant mice with decreased PP_i concentrations and hypercementosis would affect periodontal remodeling, reducing cementum resorption that arises as an unwanted consequence of OTM. We used a novel orthodontic model in *Enpp1* mutant mice to analyze OTM, periodontal remodeling, osteoclast response, and tooth root resorption.

Materials and Methods

Mice

Animal experiments were approved by the National Institute of Arthritis and Musculoskeletal and Skin Diseases (NIAMS) Animal Care and Use Committee. Two lines of *Enpp1* mutant mice were used in the current study (Jackson Labs). Phenotyping and genotyping have been previously described for $Enpp1^{asj}$ (C57BL/6J-$Enpp1^{asj}$/GrsrJ) mice (Li et al. 2013) and for $Enpp1^{asj\text{-}2J}$ (BALB/cJ-$Enpp1^{asj\text{-}2J}$/GrsrJ) mice (Li et al. 2014). Both lines harbor *Enpp1* loss-of-function mutations causing 80% reduced plasma PP_i and hypermineralization (Li et al. 2013; McKee et al. 2013; Li et al. 2014). *Enpp1* mutant mice were compared to littermate wild-type (WT) mice. Mice were fed standard rodent chow and provided access to water ad libitum. One cohort (3 WT and 4 $Enpp1^{asj}$ mice, including males and females) was analyzed without treatment at 60 d postnatal (dpn), while another cohort of $Enpp1^{asj\text{-}2J}$ mice underwent OTM.

Orthodontic Tooth Movement

At 60 dpn, isoflurane-anesthetized WT and $Enpp1^{asj\text{-}2J}$ mice (5/group, including males and females) were fixed with an orthodontic appliance according to a modified method described previously for rats (Ong et al. 2000; Zhang et al. 2003; Jäger et al. 2005). The appliance consisted of a stretched closed-coil spring (0.012-inch nickel-titanium wire; Dentaline GmbH) ligated between the maxillary left first molar and maxillary incisors using dental composite restoration (Fig. 1). A split-mouth design employed right maxillary first molars as contralateral controls (CCs). The appliance delivered 0.5 N of force in the mesial/anterior direction, causing mesial tipping of the first molar. After the 11-d experimental period, animals were euthanized by CO_2. Crania were harvested and fixed in 4% paraformaldehyde (Lux et al. 2009).

Micro–Computed Tomography

Samples were scanned in a μCT 50 (Scanco Medical) at 70 kVp, 76 μA, 0.5 Al filter, 300- to 900-ms integration time, and 6- to 17-μm voxel dimension. DICOM files were exported, and reconstructed images were analyzed using Amira (version 6.1.2; FEI, Berlin) or AnalyzePro (version 1.0; AnalyzeDirect). Detailed methods for micro–computed tomography (CT) analyses and description of terms are included in the Appendix, and regions of interest (ROI) for analysis are shown in Appendix Figure 1.

Histology

Crania were fixed, hemisected, decalcified, and processed for paraffin histology, and 2- to 5-μm serial sagittal sections were prepared for hematoxylin and eosin (H&E) staining (Götz et al. 2006). Tartrate-resistant acid phosphatase (TRAP) staining was performed to identify osteoclast/odontoclast-like cells (Foster et al. 2017). Two micrographs of molar roots were randomly selected from each animal for resorption measurements.

Resorption depths (μm) into cementum and dentin in compression zones were quantified using a modification of a previously described method (Lu et al. 1999). Compression zones were located mesio-coronally to the molar root as previously described (Kawarizadeh et al. 2004; Kawarizadeh et al. 2005).

In Situ Hybridization and Immunohistochemistry

In situ hybridization (ISH) with probes for *Spp1, Tnfsf11, Mcsf1*, and *Vegf* was performed on deparaffinized sections and visualized with fast red dye (Advanced Cell Diagnostics), as previously described (Zweifler et al. 2016). Immunohistochemistry (IHC) was performed on deparaffinized sections using an avidin-biotinylated peroxidase (ABC)–based kit with a 3-amino-9-ethylcarbazole (AEC) substrate (Vector Labs, Burlingame) to produce a red-brown product. Primary antibodies included polyclonal rabbit anti-mouse osteopontin (OPN) IgG (Dr. Larry Fisher, NIDCR) and polyclonal rabbit anti-human receptor-activator of NF-kB ligand (RANKL) IgG (Novus Biologicals).

Statistical Analysis

Mean ± standard deviation (SD) are shown in graphs. Data were analyzed using an independent samples *t* test or 1-way analysis of variance (ANOVA) with post hoc Tukey test (Prism version 6.01; GraphPad Software), where $P < 0.05$ was considered statistically significant.

Results

Altered Periodontium in Enpp1 *Mutant Mice*

Enpp1^{asj} mice carry loss-of-function mutations causing 80% reduced plasma PP_i and hypermineralization (Li et al. 2013). They exhibit an identical hypercementosis phenotype previously reported in *Enpp1*$^{-/-}$ and *Enpp1*$^{ttw/ttw}$ mutant mice (Fig. 2A, B and Appendix Fig. 2) (Nociti et al. 2002; Foster et al. 2012; Zweifler et al. 2015). In a recent study (Thumbigere-Math et al. 2018), micro-CT revealed a 4-fold increased acellular cementum thickness, a 5-fold increased acellular cementum volume, and 50% increased cellular cementum volume in 12-wk *Enpp1*^{asj} versus WT mice. However, the status of other periodontal tissues (PDL and alveolar bone) was not previously analyzed in detail for *Enpp1*^{asj} or other *Enpp1* loss-of-function mice. Because of the significance of periodontal structures and their alterations to the planned orthodontic experiments, we performed high-resolution micro-CT analysis of mandibular bone and PDL space in untreated *Enpp1*^{asj} versus WT mice at 60 dpn (Fig. 2C–E). While alveolar bone volume showed no significant differences between genotypes, mandibular basal bone volume was increased 20% ($*P = 0.01$) in *Enpp1*^{asj} versus WT mice (Fig. 2F, G). No significant differences ($P = 0.66$) were found in bone density between groups (Appendix Fig. 3A). Despite featuring expanded cementum, *Enpp1*^{asj} first molars displayed 20% increased ($*P = 0.01$) PDL volume (Fig. 2H), with no differences in PDL density (Appendix Fig. 3B). We reasoned that increased PDL space reflected an enlarged tooth socket and overall larger PDL interface with both bone and tooth root surfaces. Measurement of this entire PDL surface area (SA; including inner and outer PDL surfaces) revealed a significant 15% increase ($**P = 0.002$) in *Enpp1*^{asj} versus WT mice (Fig. 2I). To explore these differences in a more defined anatomical region, we identified a 300-μm ROI midway from the cementum-enamel junction to apex around the mesial root (Fig. 2J–M). Compared to WT, *Enpp1*^{asj} mice displayed significantly increased PDL thickness (10%; $**P = 0.009$) and PDL-bone/tooth SA (28%; $***P = 0.0001$) (Fig. 2J, K) within this ROI. Separating bone and tooth sides in the ROI confirmed that SA for both bone-PDL and cementum-PDL was significantly increased in *Enpp1*^{asj} versus WT mice (15% and 21%, respectively; $**P = 0.004$ and $***P = 0.0004$, respectively) (Fig. 2L, M).

Reduced OTM in Enpp1 *Mutant Mice*

Enpp1$^{asj\text{-}2J}$ mice are allelic with *Enpp1*^{asj} mice, with both featuring ENPP1 loss of function, 80% reduced plasma PP_i, and hypermineralization (Li et al. 2014). Orthodontic appliances were placed in 60 dpn WT and *Enpp1*$^{asj\text{-}2J}$ mice. All animals ($n = 5$/genotype) completed 11-d experiments in good health with orthodontic appliances intact. In all mice, orthodontic force application resulted in observable mesial movement of maxillary first molars on OTM sides. Compared to WT, *Enpp1*$^{asj\text{-}2J}$ mice displayed reduced tooth movement (Fig. 3A–F) and increased vertical alveolar bone loss (Fig. 3G, H). Quantitative analysis confirmed a 38% reduction ($*P = 0.02$) in mesial tooth movement (Fig. 3I) and 50% greater bone loss on the OTM side of *Enpp1*$^{asj\text{-}2J}$ versus WT mice, a trend that did not reach statistical significance ($P = 0.12$) (Fig. 3J). Untreated CC sides showed no differences between groups (Appendix Fig. 4).

To provide further insights into altered tooth movement, PDL and bone in compression (mesial) and tension (distal) zones around molars on OTM sides were assessed and compared to the same anatomic regions on CC sides. One *Enpp1*$^{asj\text{-}2J}$ maxillary CC side was removed from analysis due to suspected periodontitis secondary to food impaction. In OTM sites, *Enpp1*$^{asj\text{-}2J}$ mice showed no differences in alveolar bone density in either compression ($P = 0.24$) or tension zones ($P = 0.67$) compared to WT mice (Fig. 4A). However, mean PDL width on mesial aspects of OTM sites was greater ($*P = 0.02$) in *Enpp1*$^{asj\text{-}2J}$ than WT molars, while on the distal (tension) side, *Enpp1*$^{asj\text{-}2J}$ molars exhibited a nonsignificant ($P = 0.12$) trend of decreased PDL width (Fig. 4B). When changes in PDL width were calculated as differences between OTM and CC sides (i.e., $\Delta\,[PDL_{OTM} - PDL_{CC}]$), *Enpp1*$^{asj\text{-}2J}$ molars displayed trends indicating less change on both mesial and distal aspects (Fig. 4C), suggesting they were less responsive to orthodontic forces than WT mice.

Reduced Dentin Resorption in Orthodontically Treated Enpp1 *Mutant Mice*

Reduced tooth movement in *Enpp1*$^{asj\text{-}2J}$ versus WT mice suggested altered osteoclast response, prompting examination of

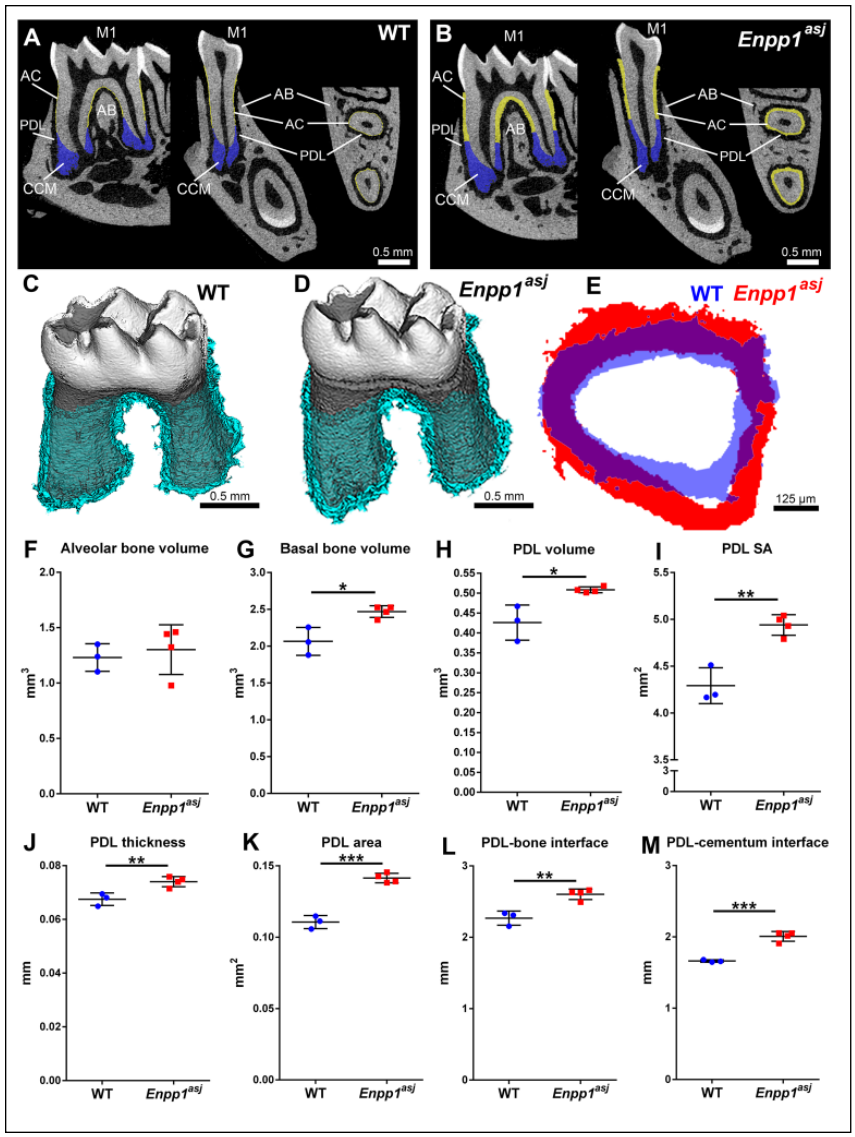

Figure 2. Altered periodontium in *Enpp1* mutant mice. (**A, B**) Two-dimensional micro–computed tomography (CT) reconstructions of wild-type (WT) and *Enpp1*^{asj} mouse mandibles highlighting the mandibular first molar (M1) in sagittal, coronal (buccal-lingual), and transverse planes (respectively, left to right). Acellular cementum (AC) is highlighted in yellow and cellular cementum (CCM) is highlighted in blue. Note the dramatically expanded AC in *Enpp1*^{asj} mice versus WT, although the periodontal ligament (PDL) space is maintained between M1 and alveolar bone (AB). (**C, D**) Three-dimensional micro-CT reconstructions of WT and *Enpp1*^{asj} mandibular molars separated from alveolar bone socket. Segmented PDL space around molar roots is highlighted light blue. (**E**) Overlay of PDL thickness from M1 mesial roots shows that *Enpp1*^{asj} PDL (red) is maintained and expanded over WT PDL (blue). (**F**) Alveolar bone volume shows no significant differences between WT and *Enpp1*^{asj} mice. (**G**) Basal bone volume is significantly increased (**P* = 0.01) in *Enpp1*^{asj} versus WT mice. (**H**) *Enpp1*^{asj} mice display a significant (**P* = 0.01) increase in PDL volume around the first molar. (**I**) Surface area (SA) of PDL interface with bone and tooth is significantly (***P* = 0.002) increased in *Enpp1*^{asj} versus WT mice. Using a 50-slice (300-µm) region of interest midway down the mesial molar root, *Enpp1*^{asj} mice display (**J**) significantly increased PDL thickness (***P* = 0.009) and (**K**) significantly increased PDL-bone/tooth SA (****P* = 0.0001) compared to WT controls. Separating the bone and tooth sides of the PDL interface confirms (**L**) significantly increased bone-PDL surface SA (***P* = 0.004) and (**M**) cementum-PDL SA (****P* = 0.0004) compared to WT controls.

tooth and bone resorption. Loading forces induced root resorption in both WT and *Enpp1*$^{asj\text{-}2J}$ mice, evident as resorption lacunae in compression zones of OTM sites (Fig. 4D). When average resorption depths were compared, no difference was found between WT and *Enpp1*$^{asj\text{-}2J}$ mice ($P = 0.92$) (Fig. 4E). However, differences were noted when resorption depths were separated for cementum and dentin. While resorption in WT was observed in both cementum and dentin, resorption in *Enpp1*$^{asj\text{-}2J}$ mice was almost entirely limited to cementum (Fig. 4F–J). *Enpp1*$^{asj\text{-}2J}$ mice featured 150% increased cementum resorption ($P = 0.003$) and 92% decreased dentin resorption ($P < 0.0001$) (Fig. 4F).

Altered Osteoclast Distribution in Orthodontically Treated Enpp1 *Mutant Mice*

Based on reduced tooth movement and dentin resorption in *Enpp1*$^{asj\text{-}2J}$ mice versus WT, we analyzed number and distribution of TRAP-positive osteoclast/odontoclast-like cells in periodontal tissues (Fig. 4K, L). On the CC side, *Enpp1*$^{asj\text{-}2J}$ mice featured a nonsignificant 26% increase in the number of TRAP-positive cells ($P = 0.09$) (Fig. 4M). On the OTM side, *Enpp1*$^{asj\text{-}2J}$ mice exhibited a significant 64% reduction (**P* = 0.04) in TRAP-positive cells versus WT. TRAP-positive cell counts separated by cementum type revealed no significant differences in numbers on the acellular cementum, but OTM sites showed an increased mean number of osteoclasts/odontoclasts in both WT and *Enpp1*$^{asj\text{-}2J}$ mice (Fig. 4N). There was no difference in TRAP-positive cells on the cellular cementum of *Enpp1*$^{asj\text{-}2J}$ versus WT mice on the CC side, but OTM sites showed increased osteoclast-like cells in WT but not *Enpp1*$^{asj\text{-}2J}$ mouse cellular cementum (Fig. 4O).

Focusing only on OTM compression zones, we noted an 85% reduction in TRAP-positive cells on alveolar bone surfaces (****P* < 0.0001) and more than a 200% increase in TRAP-positive cells on root surfaces (**P* = 0.01) of *Enpp1*$^{asj\text{-}2J}$ versus WT mice (Fig. 4P). Whereas WT mice featured greater numbers of osteoclast-like cells on bone versus tooth root surfaces (5.3 vs. 0.9 cells, respectively), this trend was inverted in *Enpp1*$^{asj\text{-}2J}$ mice, where alveolar bone harbored fewer TRAP-positive cells than root surfaces (0.8 vs. 3.1 cells, respectively).

Regulators of osteoclast/odontoclast migration/attachment (*Spp1*/OPN, *Vegf*) and differentiation (*Tnfsf11*/RANKL, *Mcsf1*) were assessed. ISH in preoperative 60 dpn mandibular molars showed increased *Spp1* messenger RNA (mRNA) in *Enpp1*$^{asj\text{-}2J}$ cementoblasts compared to WT (Appendix Fig. 5A–C). IHC identified intense OPN immunolocalization in *Enpp1*$^{asj\text{-}2J}$ acellular cementum and associated cementocyte-like cells and lining cementoblasts in mesial regions of maxillary molars on both CC and OTM (compression) sides compared to WT, while alveolar bone OPN labeling was similar between genotypes and locations (Fig. 5A–D). *Tnfsf11* mRNA was not found in association with preoperative dental or periodontal cells in *Enpp1*$^{asj\text{-}2J}$ or WT mice (Appendix Fig. 5D–F). However, RANKL immunolocalization was associated with sites of bone/tooth resorption on OTM sides of *Enpp1*$^{asj\text{-}2J}$ and WT mice (Fig. 5E–H). Positive RANKL staining was observed in some cementocyte-like cells in *Enpp1*$^{asj\text{-}2J}$ mice, as well as in osteocytes of both genotypes. *Mcsf1* and *Vegf* mRNAs were not found in association with preoperative *Enpp1*$^{asj\text{-}2J}$ or WT molars (Appendix Fig. G–L).

Discussion

To our knowledge, this is the first study focused on effects of orthodontic force on periodontal tissues in genetically altered mice harboring substantially altered cementum and periodontal structures. *Enpp1* mutant mice feature decreased PP_i, leading to significantly increased acellular cementum and expanded PDL volume with larger PDL-bone and PDL-tooth surface areas. *Enpp1* mutant mice undergoing OTM exhibited reduced tooth movement, less evidence of PDL compression, reduced dentin but increased cementum resorption, and altered distribution of osteoclasts/odontoclasts on root and bone surfaces compared to WT mice. While the hypothesis of reduced cementum resorption in *Enpp1* mutant mice undergoing OTM was not validated, observations of decreased tooth movement and altered osteoclast/odontoclast distribution provide novel insights into the intersection of mineral metabolism and periodontal remodeling.

ENPP1 is a regulator of extracellular levels of PP_i, an inhibitor of physiological and pathological mineralization (Millán 2013). ENPP1 is selectively highly expressed by cementoblasts during acellular cementum formation, and *Enpp1* loss of function in mice causes increased acellular cementum thickness (Nociti et al. 2002; Foster et al. 2012; Zweifler et al. 2015). In mice, *Ank* loss of function also reduces PP_i levels, resulting in hypercementosis (Nociti et al. 2002; Foster et al. 2012). We have identified targeted PP_i depletion as a novel approach to promote cementum regeneration using a surgical defect model (Rodrigues et al. 2011). Because cementum is a target of undesirable root resorption resulting from OTM, we aimed to understand whether altered PP_i metabolism and/or periodontal and cementum properties would prove beneficial in this context. The OTM model employed has been characterized as a reliable approach for studying periodontal remodeling induced by compression and tension, producing well-described changes in mesial tooth movement, alveolar bone height, osteoclast regulation, and root resorption (Ong et al. 2000; Pavlin et al. 2000a, 2000b; Jäger et al. 2005; Nakamura et al. 2008; Gonzales et al. 2009; Kitaura et al. 2009; Wolf et al. 2013; Wolf et al. 2014).

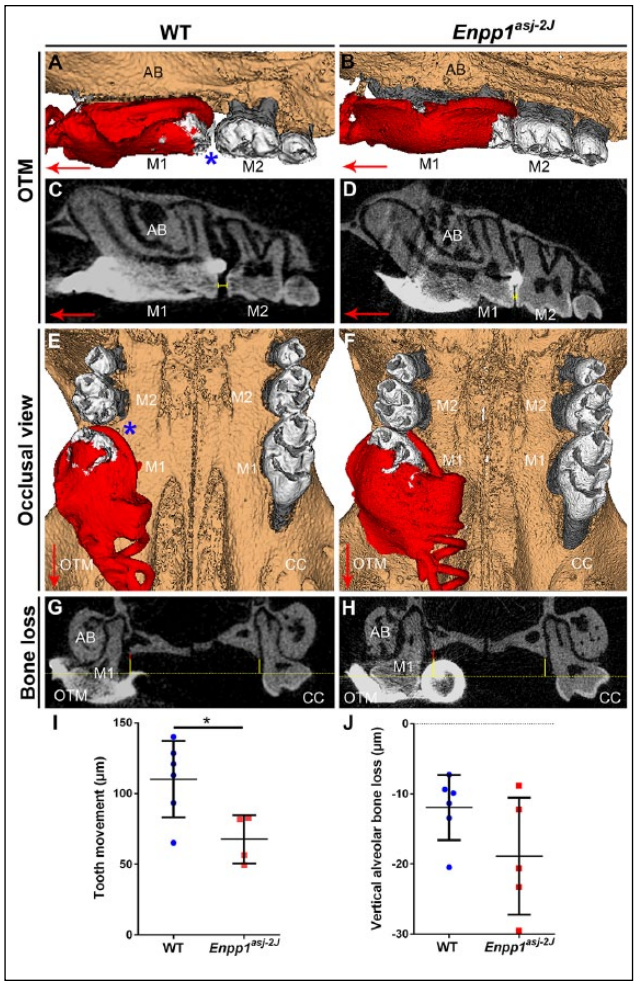

Figure 3. Reduced orthodontic tooth movement in *Enpp1* mutant mice. Three-dimensional and 2-dimensional micro–computed tomography (CT) reconstructions of mouse maxillary molars under orthodontic tooth movement (OTM) or on contralateral control (CC) sides. (**A–D**) Compared to wild-type (WT) controls (left column), *Enpp1*$^{asj\text{-}2J}$ mice (right column) display reduced mesial movement of the first maxillary molar (M1) on the OTM side. Displacement of M1 from contact with the second molar (M2) is indicated by a blue asterisk in A and yellow bracket in C. (**E, F**) Occlusal view displaying both OTM and CC sides, with the blue asterisk indicating greater separation between M1 and M2 in WT mice. Large red arrows in panels A to F indicate mesial direction. Panels A, B, E, and F show coil and composite in red color. (**G, H**) Coronal micro-CT section showing alveolar bone (AB) height around M1. Yellow-dotted line indicates plane of cemento-enamel junction (CEJ) of M1 lingual aspects, while solid yellow line shows vertical distance of CEJ to alveolar bone crest (ABC). On the OTM side, additional CEJ-ABC distance over that of the CC side is indicated by a solid red vertical line. (**I**) Linear measurements reveal a significant (*P = 0.02) 38% reduction in mesial tooth movement on the OTM sides of *Enpp1*$^{asj\text{-}2J}$ versus WT mice. (**J**) *Enpp1*$^{asj\text{-}2J}$ mice display a mean 50% increased vertical alveolar bone loss around M1 in the OTM group, a trend that did not reach the level of significance (P = 0.12).

We discovered significantly reduced tooth movement in *Enpp1* mutant versus WT mice. Several hypotheses present themselves based on previous findings and data reported here.

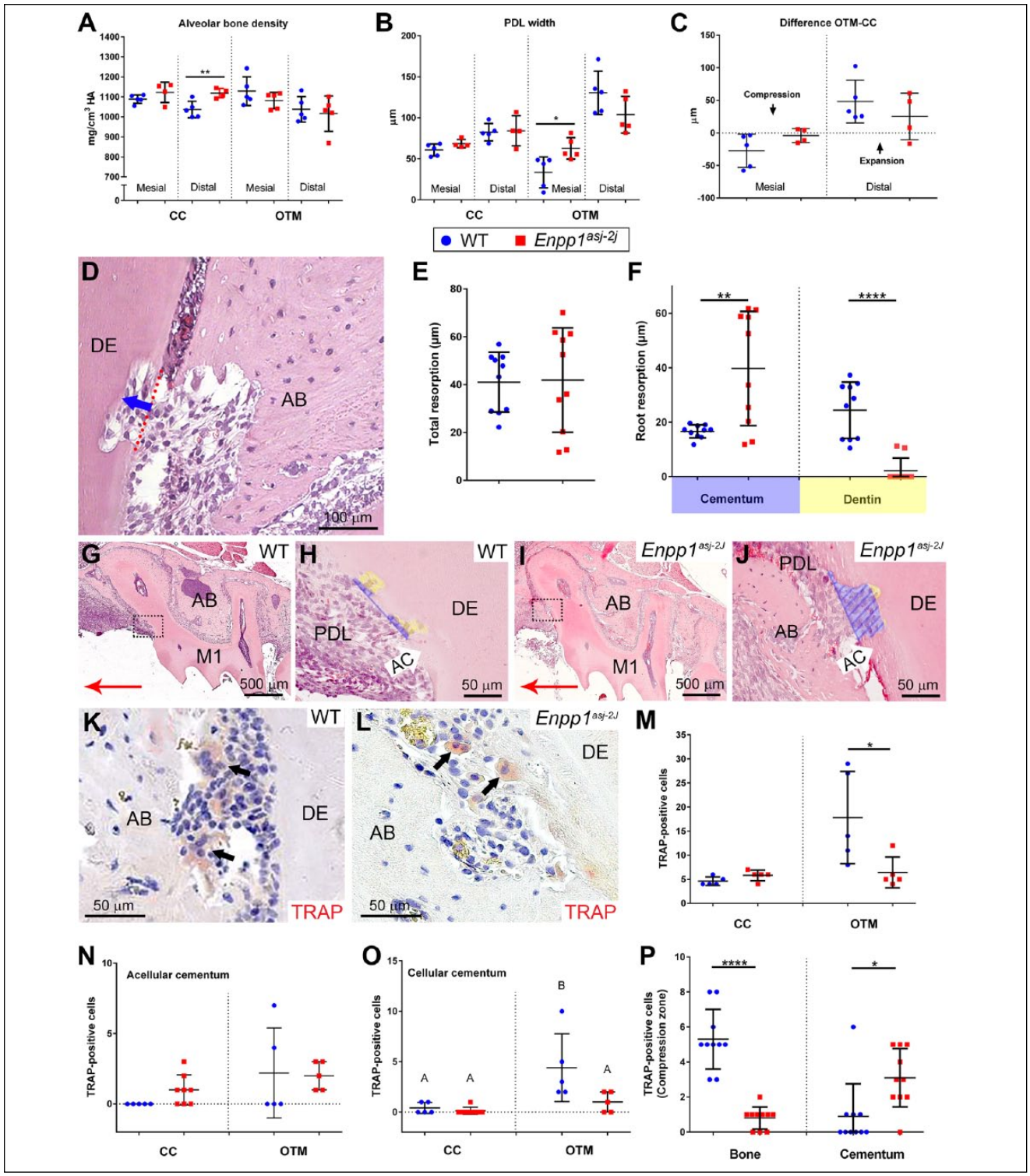

Figure 4. Altered periodontal parameters, resorption, and osteoclast distribution in *Enpp1* mutant mice under orthodontic loading. (**A**) Alveolar bone (AB) densities on mesial and distal aspects of the contralateral control (CC) roots display mean increases in *Enpp1*$^{asj\text{-}2J}$ (red squares) versus wild-type (WT) (blue circles) mice, although only the distal aspect is significant ($^{**}P = 0.01$). On orthodontic tooth movement (OTM) sides, *Enpp1*$^{asj\text{-}2J}$ mice showed nonsignificant mean decreases in AB density. (**B**) On CC sides, mean periodontal ligament (PDL) widths are increased in *Enpp1*$^{asj\text{-}2J}$ versus WT molars but do not reach significance ($P = 0.12$ and 0.86). On OTM sides, mesial PDL widths are significantly increased ($^{*}P = 0.02$) and distal PDL widths nonsignificantly ($P = 0.12$) decreased in *Enpp1*$^{asj\text{-}2J}$ versus WT molars. (**C**) *Enpp1*$^{asj\text{-}2J}$ PDL displays less change on both mesial and distal aspects when calculated as differences between OTM and CC sides. (**D**) Linear measurements of resorption depth into AC and dentin (DE) were made in compression zones on OTM sides. Red-dotted line indicates original surface while blue arrow shows path of depth measurement. (**E**) No mean difference ($P = 0.92$) is observed between WT and *Enpp1*$^{asj\text{-}2J}$ mice in overall resorption depth. (**F**) Separating resorption depths for AC and DE reveals

Because of the critical role of osteoclast-driven bone remodeling in OTM, potential osteoclast defects should be considered. However, normal osteoclast formation and function was reported in *Enpp1* knockout mice versus controls (Hajjawi et al. 2014). Our previous study indicated increased osteoclast numbers on alveolar bone surfaces of *Enpp1* knockout versus WT mice, allowing for bone remodeling and maintenance of PDL space despite cementum expansion (Foster et al. 2012). Three-dimensional micro-CT analyses of PDL volume and thickness reported here confirm maintenance and even expansion of PDL space. However, while *Enpp1* mutant mice showed similar or slightly greater osteoclast numbers in CC (unloaded) periodontia, total TRAP-positive cells were decreased on OTM sides. Furthermore, preference of clastic cells appeared to switch from bone to root surfaces in *Enpp1* mutant mice. While WT molars undergoing OTM presented the expected combination of dentin and cementum resorption, *Enpp1* mutant mouse molars exhibited resorption lacunae limited almost exclusively to the cementum. While one reason for this is the relative cervical cementum thickness in *Enpp1* mutant mice, it is intriguing to consider that cementum maintains a high regenerative potential, and resorptive defects in cementum are classified as less severe and more likely to spontaneously regenerate (Lossdörfer et al. 2010; Rodrigues et al. 2011).

We recently compiled the first report of cervical hypercementosis resulting from generalized arterial calcification of infancy (GACI; OMIM# 208000) in human subjects caused by *ENPP1* mutations (Thumbigere-Math et al. 2018). Intriguingly, several GACI patients exhibited dental infraocclusion (lack of normal eruption/maintenance of occlusal position), failure of primary tooth exfoliation, ankylosis, and/or unusual reparative cementum on primary tooth roots. One GACI subject's dental history highlighted difficulty in achieving OTM. In all of these manifestations, altered regulation of mineralization (e.g., ankylosis) and/or resorption may be suspected. While defective osteoclast/odontoclast resorption has not been previously documented in *Enpp1* loss-of-function mice or GACI subjects, loss of function of PP_i regulator ANK/ANKH contributes to osteoclast dysfunction in craniometaphyseal dysplasia (Chen et al. 2014). These findings implicating altered osteoclast/odontoclast activities in mice and humans with ENPP1 loss of function warrant further investigation.

Additional hypotheses for altered OTM in *Enpp1* mutant mice may involve the unusual inclusion of cementocyte-like cells in the thick cervical cementum that under normal conditions remains acellular. Some of these unusually located cementocytes express RANKL, possibly promoting migration and activation of osteoclast precursors to root rather than bone surfaces. We show increased expression of *Spp1*/OPN in cementoblasts and cervical cementocytes of *Enpp1*^{asj} versus WT mice. OPN is an extracellular matrix protein that promotes cell migration and attachment, and absence of OPN has caused defective osteoclast recruitment and reduced OTM in mice (Chung et al. 2008; Walker et al. 2010). Conversely, increased OPN expression by cementum-associated cells in *Enpp1* loss-of-function mice could influence osteoclast recruitment toward the root surface and away from bone, affecting resorptive activity at these locations. In a report on hypophosphatemic *Hyp* mutant mice, Coyac and colleagues found that increased OPN played a role in mineralization defects in dentin and alveolar bone, and sustained osteoclastic activity following ligature-induced periodontitis was associated with OPN-rich osteoid (Coyac et al. 2017). However, OPN was not localized to the hypomineralized cellular cementum. The potential for changes in inorganic phosphate and PP_i concentrations to affect osteoclasts and bone remodeling should be explored in more detail in future studies.

We propose an additional hypothesis to potentially explain reduced OTM in *Enpp1* mutant mice. Micro-CT analysis revealed increased PDL volume and thickness, as well as nearly 30% increased surface area between PDL and tooth root/alveolar bone of *Enpp1* mutant versus WT mice. These interfaces incorporate high-density Sharpey's fiber insertions into both cementum and bone surfaces. Assuming the density of Sharpey's fibers remains similar, this translates to an increase of almost 30% more inserted fibers in *Enpp1* mutant mice. This altered periodontal attachment would be anticipated to increase the strength of PDL-bone/tooth attachment, affecting both mechanical deformation of PDL and periodontal remodeling, which may be observed as a reduced response to orthodontic loading. *Enpp1* mutant mouse molars exhibited less compression and expansion than similarly loaded WT molars. Less compression mesial to the root would be expected to produce less vascular disturbance and attract fewer osteoclast precursors, and *Enpp1* mutant mice exhibited fewer osteoclasts on OTM sides. While speculative, this observation of altered periodontal structure in *Enpp1* mutant mice may explain reduced deformation under mechanical stress, reduced tooth movement, and fewer osteoclasts, as well as altered tooth movement and delayed primary tooth exfoliation in GACI subjects (Thumbigere-Math et al. 2018). Mechanical testing of *Enpp1* mutant periodontia may provide further insights.

a 150% increase in AC resorption (**P = 0.003) and a 92% decrease in DE resorption (****P < 0.0001) in *Enpp1*$^{asj\text{-}2J}$ versus WT mice. (**G–J**) Histological images of resorption in AC (blue shading) and DE (yellow shading) in compression zones (boxes in G and I) of WT and *Enpp1*$^{asj\text{-}2J}$ mice. Red arrows in G and I indicate mesial direction. Focusing on compression zones of M1 distal roots, numbers and distribution of tartrate-resistant acid phosphatase (TRAP)–positive osteoclast/odontoclast-like cells (black arrows) were counted in (**K**) WT and (**L**) *Enpp1*$^{asj\text{-}2J}$ mice. (**M**) On CC sides, the baseline number of TRAP-positive cells is not significantly different (P = 0.09), while on the OTM side, *Enpp1*$^{asj\text{-}2J}$ mice exhibit a significant (*P = 0.04) 64% reduction in TRAP-positive cells compared to WT. (**N**) No significant differences in TRAP-positive cells are observed on AC surfaces of WT versus *Enpp1*$^{asj\text{-}2J}$ mice. (**O**) No differences in TRAP-positive cells are found on cellular cementum (CCM) of WT versus *Enpp1*$^{asj\text{-}2J}$ mice on the CC side, but OTM induces increased osteoclast-like cells on WT CCM but not *Enpp1*$^{asj\text{-}2J}$ CCM. In panel L, different capital letters indicate significant differences (P < 0.05) between means. (**P**) Separating TRAP-positive cells by localization to AB or cementum surfaces reveals a significant (****P < 0.0001) 85% reduction in TRAP-positive cells on AB surfaces and a 200% increase (*P = 0.01) in TRAP-positive cells on root surfaces in *Enpp1*$^{asj\text{-}2J}$ versus WT mice.

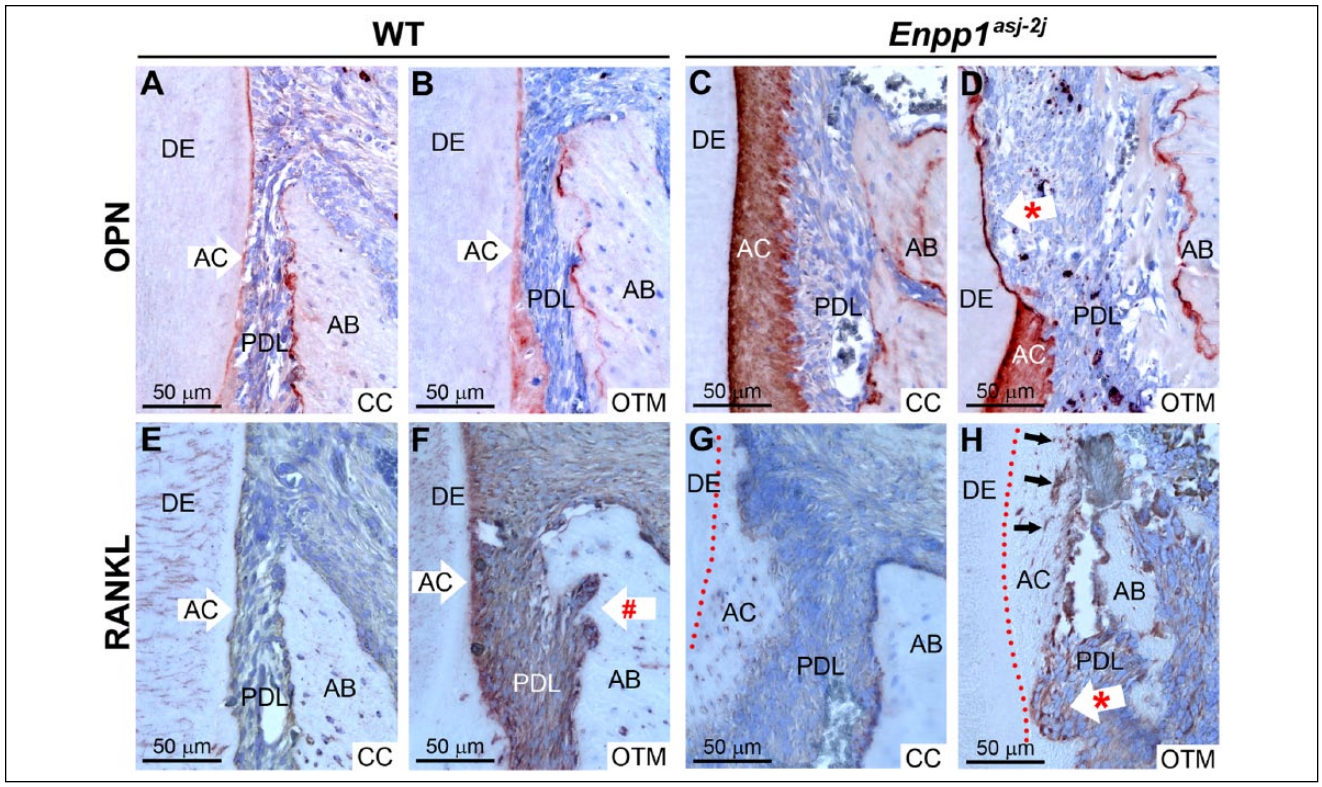

Figure 5. Altered immunostaining of osteopontin and receptor-activator of NF-κB ligand (RANKL) in *Enpp1* mutant mice. Immunohistochemistry (IHC) identified osteopontin (OPN) in wild-type (WT) acellular cementum (AC) and alveolar bone (AB) on (**A**) contralateral control (CC) and (**B**) orthodontic tooth movement (OTM) sides. *Enpp1*$^{asj-2J}$ mice featured intense OPN localization in their expanded AC of both (**C**) CC and (**D**) OTM sides. Asterisk (*) in D indicates tooth root resorption. (**E**, **F**) In WT mice, more intense RANKL immunolocalization was observed at sites of active bone resorption (indicated by # in F) and in some nearby osteocytes on OTM sides. (**G**, **H**) In *Enpp1*$^{asj-2J}$ mice, more intense RANKL staining was observed at sites of bone and tooth resorption (indicated by * in H) and in some cementocyte-like cells in the expanded AC layer (black arrows in H). Red-dotted lines in G and H indicate border of AC and dentin (DE).

Author Contributions

M. Wolf, V. Thumbigere-Math, B.L. Foster, contributed to conception, design, data acquisition, analysis, and interpretation, drafted and critically revised the manuscript; M. Ao, contributed to data acquisition, critically revised the manuscript; M.B. Chavez, T.N. Kolli, contributed to data acquisition, analysis, and interpretation, drafted and critically revised the manuscript; K. Becker, contributed to conception and data interpretation, critically revised the manuscript; E.Y. Chu, contributed to data acquisition and analysis, critically revised the manuscript; A. Jäger, contributed to data acquisition, analysis, and interpretation, critically revised the manuscript; M.J. Somerman, contributed to conception, design, data analysis and interpretation, critically revised the manuscript. All authors gave final approval and agree to be accountable for all aspects of the work.

Acknowledgments

This research was supported by the German Orthodontic Association (DGKFO) and Medical Faculty University of Bonn, Germany (to M.W.); grants AR 066110 to B.L.F. and AR 069643 to V.T.-M. from the National Institute of Arthritis and Musculoskeletal and Skin Diseases (NIAMS), National Institutes of Health (NIH, Bethesda, MD); and intramural funding from NIAMS/NIH (to M.J.S). We thank Dr. Kristina Zaal (Light Imaging Section, NIAMS/NIH) for assistance in slide scanning and Alyssa Coulter (NIAMS/NIH) for assistance with histological sectioning. We thank the editor and anonymous reviewers for their critiques and suggestions that improved this manuscript. The authors declare no potential conflicts of interest with respect to the authorship and/or publication of this article.

References

Bosshardt DD, Sculean A. 2009. Does periodontal tissue regeneration really work? Periodontol 2000. 51:208–219.

Chen IP, Tadinada A, Dutra EH, Utreja A, Uribe F, Reichenberger EJ. 2014. Dental anomalies associated with craniometaphyseal dysplasia. J Dent Res. 93(6):553–558.

Chung C, Soma K, Rittling S, Denhardt D, Hayata T, Nakashima K, Ezura Y, Noda M. 2008. OPN deficiency suppresses appearance of odontoclastic cells and resorption of the tooth root induced by experimental force application. J Cell Physiol. 214(3):614–620.

Coyac BR, Falgayrac G, Baroukh B, Slimani L, Sadoine J, Penel G, Biosse-Duplan M, Schinke T, Linglart A, McKee MD, et al. 2017. Tissue-specific mineralization defects in the periodontium of the Hyp mouse model of X-linked hypophosphatemia. Bone. 103:334–346.

Foster BL, Kuss P, Yadav MC, Kolli TN, Narisawa S, Lukashova L, Cory E, Sah RL, Somerman MJ, Millán JL. 2017. Conditional Alpl ablation phenocopies dental defects of hypophosphatasia. J Dent Res. 96(1):81–91.

Foster BL, Nagatomo KJ, Nociti FH, Fong H, Dunn D, Tran AB, Wang W, Narisawa S, Millán JL, Somerman MJ. 2012. Central role of pyrophosphate in acellular cementum formation. PLoS One. 7(6):e38393.

Götz W, Kunert D, Zhang D, Kawarizadeh A, Lossdörfer S, Jäger A. 2006. Insulin-like growth factor system components in the periodontium during tooth root resorption and early repair processes in the rat. Eur J Oral Sci. 114(4):318–327.

Gonzales C, Hotokezaka H, Arai Y, Ninomiya T, Tominaga J, Jang I, Hotokezaka Y, Tanaka M, Yoshida N. 2009. An in vivo 3D micro-CT evaluation of tooth movement after the application of different force magnitudes in rat molar. Angle Orthod. 79(4):703–714.

Hajjawi MO, MacRae VE, Huesa C, Boyde A, Millan JL, Arnett TR, Orriss IR. 2014. Mineralisation of collagen rich soft tissues and osteocyte lacunae in enpp1(–/–) mice. Bone. 69:139–147.

Harmey D, Hessle L, Narisawa S, Johnson K, Terkeltaub R, Millán J. 2004. Concerted regulation of inorganic pyrophosphate and osteopontin by Akp2, Enpp1, and Ank: an integrated model of the pathogenesis of mineralization disorders. Am J Pathol. 164(4):1199–1209.

Jäger A, Radlanski RJ, Götz W. 1993. Demonstration of cells of the mononuclear phagocyte lineage in the periodontium following experimental tooth movement in the rat: an immunohistochemical study using monoclonal antibodies ED1 und ED2 on paraffin-embedded tissues. Histochemistry. 100(2):161–166.

Jäger A, Zhang D, Kawarizadeh A, Tolba R, Braumann B, Lossdörfer S, Götz W. 2005. Soluble cytokine receptor treatment in experimental orthodontic tooth movement in the rat. Eur J Orthod. 27(1):1–11.

Kawarizadeh A, Bourauel C, Götz W, Jäger A. 2005. Early responses of periodontal ligament cells to mechanical stimulus in vivo. J Dent Res. 84(10):902–906.

Kawarizadeh A, Bourauel C, Zhang D, Götz W, Jäger A. 2004. Correlation of stress and strain profiles and the distribution of osteoclastic cells induced by orthodontic loading in rat. Eur J Oral Sci. 112(2):140–147.

Kim YS, Lee YM, Park JS, Lee SK, Kim EC. 2010. SIRT1 modulates high-mobility group box 1–induced osteoclastogenic cytokines in human periodontal ligament cells. J Cell Biochem. 111(5):1310–1320.

Kitaura H, Fujimura Y, Yoshimatsu M, Eguchi T, Kohara H, Jang I, Morita Y, Yoshida N. 2009. An M-CSF receptor c-Fms antibody inhibits mechanical stress-induced root resorption during orthodontic tooth movement in mice. Angle Orthod. 79(5):835–841.

Koide M, Kinugawa S, Takahashi N, Udagawa N. 2010. Osteoclastic bone resorption induced by innate immune responses. Periodontol 2000. 54(1):235–246.

Li Q, Guo H, Chou DW, Berndt A, Sundberg JP, Uitto J. 2013. Mutant Enpp1asj mice as a model for generalized arterial calcification of infancy. Dis Model Mech. 6(5):1227–1235.

Li Q, Pratt CH, Dionne LA, Fairfield H, Karst SY, Sundberg JP, Uitto J. 2014. Spontaneous asj-2J mutant mouse as a model for generalized arterial calcification of infancy: a large deletion/insertion mutation in the Enpp1 gene. PLoS One. 9(12):e113542.

Lossdörfer S, Yildiz F, Götz W, Kheralla Y, Jäger A. 2010. Anabolic effect of intermittent PTH(1-34) on the local microenvironment during the late phase of periodontal repair in a rat model of tooth root resorption. Clin Oral Investig. 14(1):89–98.

Lu LH, Lee K, Imoto S, Kyomen S, Tanne K. 1999. Histological and histochemical quantification of root resorption incident to the application of intrusive force to rat molars. Eur J Orthod. 21(1):57–63.

Lux CJ, Ducker B, Pritsch M, Komposch G, Niekusch U. 2009. Occlusal status and prevalence of occlusal malocclusion traits among 9-year-old schoolchildren. Eur J Orthod. 31(3):294–299.

McKee MD, Hoac B, Addison WN, Barros NM, Millán JL, Chaussain C. 2013. Extracellular matrix mineralization in periodontal tissues: noncollagenous matrix proteins, enzymes, and relationship to hypophosphatasia and X-linked hypophosphatemia. Periodontol 2000. 63(1):102–122.

Millán JL. 2013. The role of phosphatases in the initiation of skeletal mineralization. Calcif Tissue Int. 93(4):299–306.

Nakamura Y, Noda K, Shimoda S, Oikawa T, Arai C, Nomura Y, Kawasaki K. 2008. Time-lapse observation of rat periodontal ligament during function and tooth movement, using microcomputed tomography. Eur J Orthod. 30(3):320–326.

Nociti FH Jr, Berry JE, Foster BL, Gurley KA, Kingsley DM, Takata T, Miyauchi M, Somerman MJ. 2002. Cementum: a phosphate-sensitive tissue. J Dent Res. 81(12):817–821.

Ong CK, Walsh LJ, Harbrow D, Taverne AA, Symons AL. 2000. Orthodontic tooth movement in the prednisolone-treated rat. Angle Orthod. 70(2):118–125.

Pavlin D, Goldman ES, Gluhak-Heinrich J, Magness M, Zadro R. 2000a. Orthodontically stressed periodontium of transgenic mouse as a model for studying mechanical response in bone: the effect on the number of osteoblasts. Clin Orthod Res. 3(3):55–66.

Pavlin D, Goldman ES, Gluhak-Heinrich J, Magness M, Zadro R. 2000b. Orthodontically stressed periodontium of transgenic mouse as a model for studying mechanical response in bone: the effect on the number of osteoblasts. Clin Orthod Res. 3(2):55–66.

Rodrigues TL, Nagatomo KJ, Foster BL, Nociti FH, Somerman MJ. 2011. Modulation of phosphate/pyrophosphate metabolism to regenerate the periodontium: a novel in vivo approach. J Periodontol. 82(12):1757–1766.

Thumbigere-Math V, Alqadi A, Chalmers NI, Chavez MB, Chu EY, Collins MT, Ferreira CR, FitzGerald K, Gafni RI, Gahl WA, et al. 2018. Hypercementosis associated with ENPP1 mutations and GACI. J Dent Res. 97(4):432–441.

Walker CG, Dangaria S, Ito Y, Luan X, Diekwisch TG. 2010. Osteopontin is required for unloading-induced osteoclast recruitment and modulation of RANKL expression during tooth drift-associated bone remodeling, but not for super-eruption. Bone. 47(6):1020–1029.

Wolf M, Lossdörfer S, Abuduwali N, Jäger A. 2013. Potential role of high mobility group box protein 1 and intermittent PTH (1-34) in periodontal tissue repair following orthodontic tooth movement in rats. Clin Oral Investig. 17(3):989–997.

Wolf M, Lossdörfer S, Küpper K, Jäger A. 2014. Regulation of high mobility group box protein 1 expression following mechanical loading by orthodontic forces in vitro and in vivo. Eur J Orthod. 36(6):624–631.

Wolf M, Lossdörfer S, Römer P, Kirschneck C, Küpper K, Deschner J, Jäger A. 2016. Short-term heat pre-treatment modulates the release of HMGB1 and pro-inflammatory cytokines in hPDL cells following mechanical loading and affects monocyte behavior. Clin Oral Investig. 20(5):923–931.

Yamaguchi M, Aihara N, Kojima T, Kasai K. 2006. Rankl increase in compressed periodontal ligament cells from root resorption. J Dent Res. 85(8):751–756.

Zhang D, Goetz W, Braumann B, Bourauel C, Jaeger A. 2003. Effect of soluble receptors to interleukin-1 and tumor necrosis factor alpha on experimentally induced root resorption in rats. J Periodontal Res. 38(3):324–332.

Zweifler LE, Ao M, Yadav M, Kuss P, Narisawa S, Kolli TN, Wimer HF, Farquharson C, Somerman MJ, Millán JL, et al. 2016. Role of phospho1 in periodontal development and function. J Dent Res. 95(7):742–751.

Zweifler LE, Patel MK, Nociti FH Jr, Wimer HF, Millán JL, Somerman MJ, Foster BL. 2015. Counter-regulatory phosphatases TNAP and NPP1 temporally regulate tooth root cementogenesis. Int J Oral Sci. 7(1):27–41.